Application of MIVM for Sn-Zn System in Vacuum Distillation

LINGXIN KONG, BIN YANG, BAOQIANG XU, YIFU LI, YUANSHOU HU, and DACHUN LIU

The activities of components of Sn-Zn system were predicted based on the molecular interaction volume model (MIVM). The separation coefficients and the vapor–liquid phase equilibrium of Sn-Zn system were also predicted using the MIVM. The predicted results indicated that the content of tin in the vapor phase was 0.000052 wt pct, while in the liquid phase, it was 99.98 wt pct at 1173 K (900 °C). Experimental investigations into the separation of Sn-Zn alloy by vacuum distillation were carried out for the proper interpretation of the predicted results. The effects of vacuum level (15 to 200 Pa), distillation temperatures [873 K to 1273 K (600 °C to 1000 °C)], and soaking time (20 to 60 minutes) were studied. The experimental results indicated that the content of tin in the vapor phase was 0.001 wt pct, while in the liquid phase, it was 99.98 wt pct at 1173 K (900 °C). The experimental results match well with the predicted data, suggesting that the MIVM is a suitable model for Sn-Zn system.

I. INTRODUCTION

TIN is an indispensable metal, which was widely used in solder, tin plate and bearings. More recently, the application of tin in electronic, electrical, and various engineering achievements has been considerably increased.[1] Zinc is usually employed for surface corrosion-protective, coating, and planting process materials and for making compound semiconductors such as ZnSe for blue light emitting diodes, CdZnTe for detectors, ZnTe for thermo-electric cooling devices, and the application range of Zn has also been increased and broadened greatly.[2,3] The decrease of natural resources, together with the increasing demand for Sn and Zn, has encouraged the recycling and separation of waste Sn-Zn alloys produced from smelteries and recycled from various industries.

Vacuum distillation is regarded as one of the most effective and environment-friendly method for metal recycling and separation.[4] It has many advantages such as short flow sheet, lower energy consumption, *etc*. Above all, vacuum distillation can eliminate the disadvantages of traditional metallurgical processes and has been studied and successfully used in separation and purification of various elements from alloys.[5–9]

The thermodynamic properties of binary liquid alloys are important for understanding the process metallurgy. But the experimental thermodynamic study is very time consuming since a great number of measurements are necessary. Furthermore, the determination of thermodynamic data of binary system needs not only the excellent instruments and the consummate skill of a researcher but also the continuous financial support. Theoretical predicting, therefore, is a significant and effective approach to obtain thermodynamic properties of alloys.[10]

Han *et al.*[11] have investigated the recovery of valuable metals from Sn-Zn alloy by vacuum distillation in which Zn (99.9 wt pct) and Sn (85 wt pct) were obtained from volatile and residue, respectively, which indicates that vacuum distillation is an effective method for the separation of Sn-Zn alloy. Nevertheless, their studies have focused only on industrial experiments and have not developed appropriate theory for the proper interpretation of the experimental results. Ali *et al.*[3] have prepared the high pure zinc using the selective evaporation under vacuum where m6N pure (99.9999 pct) Zn was obtained. However, their studies have not considered the activities of components of crude zinc. Kong *et al.*[12] investigated the application of MIVM for Pb-Sn system in vacuum distillation. However, their studies focused only on the Pb-based binary alloy. Moreover, the investigation about the application of MIVM in vacuum distillation of Sn-based alloys has not been reported. The Sn-Zn alloy, therefore, was selected to demonstrate the utility of MIVM in vacuum distillation in order to provide a rigorous model for predicting quantitatively the distribution of components of Sn-Zn alloy in vacuum distillation, which will instruct the practical vacuum distillation of Sn-Zn alloy. The purpose of this study, therefore, was to predict the activities of components of Sn-Zn system. The separation coefficients and vapor–liquid phase equilibrium composition were also predicted. Experiments for the separation of Sn-Zn alloy were carried out under

LINGXIN KONG, Ph.D Candidate, BIN YANG and DACHUN LIU, Professors, BAOQIANG XU, Associate Professor, and YIFU LI, Lecturer, are with The National Engineering Laboratory for Vacuum Metallurgy, Kunming University of Science and Technology, Kunming 650093, P.R. China, also with the Key Laboratory of Vacuum Metallurgy for Nonferrous Metals of Yunnan Province, Kunming University of Science and Technology, Kunming 650093, P.R. China, and also with the State Key Laboratory of Complex Nonferrous Metal Resources Clear Utilization. Contact e-mail: kgyb2005@126.com YUANSHOU HU, Engineer, is with The National Engineering Laboratory for Vacuum Metallurgy, Kunming University of Science and Technology, and also with the Zinc Division of Yunnan Copper Industry Co., Ltd, Kunming 650102, P.R. China.
Manuscript submitted July 10, 2014.
Article published online December 5, 2014.

vacuum condition, and a comparison between the experimental results and the predicted data was also executed.

II. MODEL PREDICTION

The MIVM was obtained from the physical perspective of liquid molecular movements in which liquid molecules are not like solid atoms, which are vibrating continuously at lattice sites, and not like gas molecules, which are in continuous random motion but are migrating non-randomly from one cell to another. This indicates that the cells made up of the molecules are not the prison cages restraining themselves but are the carriers on which they are migrating.[13] More detailed fundamental basis of the MIVM is available in Reference 14

According to the above description and the statistic thermodynamics, the partition function[14] of a binary liquid mixture $i - j$ can be obtained as follows:

$$P = \frac{P_c}{N_i! \Lambda_i^{3N_i} N_j! \Lambda_j^{3N_j}}, \quad [1]$$

where N_i and $\Lambda_i^{3N_i}$ are the molecular number and the partition function of molecular kinetic energy of the pure matter i, respectively; and P_c is the configurational partition function of mixture $i - j$ and can be expressed as

$$P_c = \left(\frac{V}{N}\right)^N \exp\left(-\frac{N\varepsilon_p}{kT}\right), \quad [2]$$

where V is the volume of the mixture; k is the Boltzmann constant; T is the absolute temperature; and ε_p is the mixing potential energy function of the molecules i and j. The partition function and configurational partition function of the pure matter i and j have the similar expression as those of liquid mixture $i - j$.

According to the relationship between Gibbs energy and partition function

$$G = kT\left[V\left(\frac{\partial \ln P}{\partial V}\right)_T - \ln P\right], \quad [3]$$

one can get the Gibbs energy of a binary mixture $i - j$:

$$G = kT\left[N - N(\ln\frac{V}{N}) + \frac{N\varepsilon_p}{kT} + \ln(N_i! \Lambda_i^{3N_i} N_j! \Lambda_j^{3N_j})\right]. \quad [4]$$

The Gibbs energies of the pure matters i and j have the parallel expression as that of mixture $i - j$. A new expression of the excess Gibbs energy of mixture $i - j$, therefore, can be obtained as follows:

$$G^E = \Delta G^M - \Delta G^{idM} = (G - G^\circ) - (G_i + G_j - G^\circ)$$
$$= G - G_i - G_j \quad = nRT\left[x_i \ln\left(\frac{\Phi_i}{x_i}\right) + x_j \ln\left(\frac{\Phi_j}{x_j}\right) + \frac{\Delta\varepsilon_p}{2kT}\right], \quad [5]$$

where ΔG^M, ΔG^{idM}, and G° are the real Gibbs energy of mixing, the ideal Gibbs energy of mixing, and the

standard Gibbs energy of mixing $i - j$, respectively; x_i and x_j are the molar fractions of i and j; $\Phi_i = x_i V_{mi}/V_m$ and $\Phi_j = x_j V_{mj}/V_m$ are the molar volume fractions of components i and j in the mixture $i - j$, respectively; R is the universal constant; T is the absolute temperature; and the excess potential energy function of the mixture $i - j$ is

$$\Delta\varepsilon_p = 2\varepsilon_p - Z_i x_i \varepsilon_{ii} - Z_j x_j \varepsilon_{jj} \quad [6]$$

in which the mixing potential energy function ε_p of the molecules i and j can be chosen as

$$\varepsilon_p = \frac{1}{2}\left[Z_i x_i(x_{ii}\varepsilon_{ii} + x_{ji}\varepsilon_{ji}) + Z_j x_j(x_{jj}\varepsilon_{jj} + x_{ij}\varepsilon_{ij})\right], \quad [7]$$

where Z_i and Z_j are the nearest molecule or first coordination numbers; ε_{ii} and ε_{jj} are the i–i and j–j pair-potential energy, respectively; $\varepsilon_{ij} = \varepsilon_{ji}$.

Substituting Eqs. [6] and [7] into [5] in which Φ_i and Φ_j are replaced by local volume fractions[14] of the molecules i and j in the mixture $i - j$, the molar excess Gibbs energy $G_m^{E[14]}$ of the multicomponent can be obtained as follows:

$$\frac{G_m^E}{RT} = \sum_{i=1}^n x_i \ln\left(\frac{V_{mi}}{\sum_{j=1}^n x_j V_{mj} B_{ji}}\right)$$
$$- \frac{1}{2}\sum_{i=1}^n Z_i x_i \left(\frac{\sum_{j=1}^n x_j B_{ji} \ln B_{ji}}{\sum_{k=1}^n x_k B_{ki}}\right) = \frac{H_m^E}{RT} - \frac{S_m^E}{R}, \quad [8]$$

where V_{mi} and V_{mj} are the molar volumes of the matters i and j, respectively; and the pair-potential energy interaction parameters B_{ij} and B_{ji}[14] are defined as follows:

$$B_{ij} = \exp\left[-\left(\frac{\varepsilon_{ij} - \varepsilon_{jj}}{kT}\right)\right] \cdot B_{ji} = \exp\left[-\left(\frac{\varepsilon_{ji} - \varepsilon_{ii}}{kT}\right)\right]. \quad [9]$$

For a binary mixture i–j, with the help of the thermodynamic relation $(\partial G_m^E/\partial x_i)_{T,p,xj} = RT \ln\gamma_i$, the activity coefficients of components i and j can be derived from Eq. [8] as follows:

$$\ln\gamma_i = \ln\left(\frac{V_{mi}}{x_i V_{mi} + x_j V_{mj} B_{ji}}\right)$$
$$+ x_j\left(\frac{V_{mj}B_{ji}}{x_i V_{mi} + x_j V_{mj}B_{ji}} - \frac{V_{mi}B_{ij}}{x_j V_{mj} + x_i V_{mi}B_{ij}}\right)$$
$$- \frac{x_j^2}{2}\left(\frac{Z_i B_{ji}^2 \ln B_{ji}}{(x_i + x_j B_{ji})^2} + \frac{Z_j B_{ij} \ln B_{ij}}{(x_j + x_i B_{ij})^2}\right)$$

$$[10]$$

$$\ln\gamma_j = \ln\left(\frac{V_{mj}}{x_j V_{mj} + x_i V_{mi} B_{ij}}\right)$$
$$- x_i\left(\frac{V_{mj}B_{ji}}{x_i V_{mi} + x_j V_{mj}B_{ji}} - \frac{V_{mi}B_{ij}}{x_j V_{mj} + x_i V_{mi}B_{ij}}\right)$$
$$- \frac{x_i^2}{2}\left(\frac{Z_j B_{ij}^2 \ln B_{ij}}{(x_j + x_i B_{ij})^2} + \frac{Z_i B_{ji} \ln B_{ji}}{(x_i + x_j B_{ji})^2}\right).$$

$$[11]$$

Table I. The Infinite Dilute Thermodynamic Properties of Sn-Zn Liquid Alloy[20]

$i - j$	T (K)	$\Delta \overline{H}_i^{M\infty}$ (kJ mol^{-1})	$\overline{S}_i^{E\infty}$ (J K^{-1} mol^{-1})	$\Delta \overline{H}_j^{M\infty}$ (kJ mol^{-1})	$\overline{S}_j^{E\infty}$ (J K^{-1} mol^{-1})
Sn-Zn	750 (477 °C)	22.771	17.710	8.664	5.973

Table II. The Values of γ_i^∞, γ_j^∞, B_{ij}, and B_{ji} of Sn-Zn Alloy at the Required Temperatures

$i - j$	T [K (°C)]	γ_i^∞	γ_j^∞	B_{ij}	B_{ji}	Z_i	Z_j
Sn-Zn	750 (477)	4.578	1.956	1.0857	0.5926	6.75	9.77
	873 (600)	2.738	1.609	1.0930	0.6569	6.59	9.46
	973 (700)	1.983	1.423	1.0882	0.7131	6.48	9.25
	1073 (800)	1.526	1.288	1.0704	0.7802	6.38	9.05
	1173 (900)	1.227	1.185	1.0225	0.8807	6.29	8.87
	1273 (1000)	1.022	1.105	0.9384	1.0352	6.21	8.71

The MIVM can predict the thermodynamic properties of binary and multicomponent liquid alloys using only binary infinite dilute activity coefficients, γ_i^∞ and γ_j^∞, and more details are available in Reference 10. The prediction effect of the MIVM indicated better stability and reliability in the previous work.[15–19]

The values of B_{ij} and B_{ji} must be obtained before applying the MIVM into Sn-Zn alloy system, which can be calculated from Eq. [16] in Reference 10 using the Newton–Raphson methodology if the infinite dilute activity coefficients γ_i^∞ and γ_j^∞ are known.

The values of γ_i^∞ and γ_j^∞ at desired temperatures can be calculated from Eq. [12]:

$$\ln \gamma_i^\infty = \frac{\overline{H}_i^{E\infty}}{RT} - \frac{\overline{S}_i^{E\infty}}{R}. \qquad [12]$$

Supposing that the partial molar infinite dilute excess enthalpy $\overline{H}_i^{E\infty}$ and entropy $\overline{S}_i^{E\infty}$ of component i are independent of temperature. Then Eq. [12] may be written as

$$\ln \gamma_i^{E\infty} = \frac{a}{T} + b, \qquad [13]$$

where $a = \overline{H}_i^{E\infty}/R$ and $b = -\overline{S}_i^{E\infty}/R$, and R is the gas constant. Notice that $\overline{H}_i^{E\infty}$ is the partial molar infinite dilute mixing enthalpy of component i, viz. $\Delta \overline{H}_i^{M\infty}$. Based on Eq. [13], the infinite dilute activity coefficient γ_i^∞ at any temperature can be calculated easily from the values of $\Delta \overline{H}_i^{M\infty}$ and $\overline{S}_i^{E\infty}$ (Table I).[20] The calculated values of γ_i^∞ and γ_j^∞ at required temperatures are shown in Table II.

On the other hand, the values of B_{ij} and B_{ji} at the required temperature can be obtained from Eq. [9] in which the pair-potential energy interaction parameters $(\varepsilon_{ij} - \varepsilon_{jj})/kT$ and $(\varepsilon_{ji} - \varepsilon_{ii})/kT$ may be assumed to be independent of temperature, while the values of B_{ij} and B_{ji} are known at a certain temperature.

The required parameters B_{ij} and B_{ji} of the Sn-Zn binary alloy are shown in Table II. The values of Z_i can be calculated from Eqs. [7 through 12] in Reference 10 using the ordinary physical quantities of pure liquid metals,[21,22] as shown in Table II.

III. EXPERIMENTAL

A. Experimental Materials

The Sn-Zn alloy provided by a tin smelting company in China was chosen for the experiments. The main chemical composition of metallic elements in the Sn-Zn alloy was measured using chemical analysis method, and there was 35.7 wt pct of Sn and 64.3 wt pct of Zn in the sample.

B. Apparatus

The experiments were carried out on the self-made laboratory apparatus, as shown in Figure 1. It mainly consisted of (1) Pit furnace, (2) Evaporator—Collector set, (3) Vacuum pump, (4) Circulating water control system, and (5) Vacuum-resistance furnace (including two electrodes). A cylindrical crucible (80 mm OD × 60 mm ID × 120 mm Ht) which is made up of isostatic fine grain high-density graphite was used as the evaporator and a circular stainless steel plate (surface area = 380 cm^2) as the collector.

C. Procedures

Firstly, the graphite crucible loaded with 120 g of Sn-Zn alloy was placed at the appropriate position in the vacuum chamber, and the chamber was sealed. Next, the circular cooling water was opened, and the vacuum chamber was evacuated to a desired pressure by means of the vacuum pumping system, the chamber pressure was measured using a stand McLeod Gauge. Then the feeding material was heated to desired distillation temperatures, which was controlled by manually adjusting the furnace power input on the basis of continuous readings from mullite sheath-protected thermocouples connected to the graphite crucible. The distillation temperature could be maintained at a constant value of ±5 K (±5 °C). Zinc was evaporated in the vacuum chamber, and the volatile flowed to the cold plate which was connected to the circular cooling water, while tin was enriched in the residue. The cooled residue and the volatile were taken from the crucible and cold plate, respectively,

and weighed after the experiment was completed. The component contents in the residuals and volatiles were analyzed by flame atomic absorption spectroscopy combined with chemical analysis method.

IV. RESULTS AND DISCUSSION

A. Activities and Activity Coefficients

Substituting the corresponding parameters B_{ij} and B_{ji} into Eqs. [10] and [11], the activities of the components of Sn-Zn alloy at 750 K (477 °C) can be predicted, as
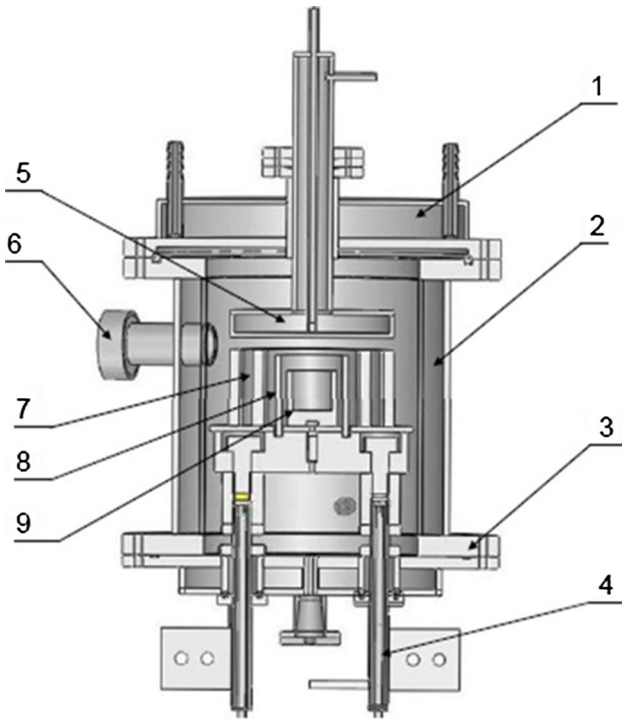

Fig. 1—Schematic diagram of the vacuum distillation experimental set-up. *1*. furnace lid; *2*. furnace body; *3*. furnace bottom; *4*. electrode; *5*. cold plate; *6*. observation door; *7*. heat holding cover; *8*. heating unit; *9*. graphite evaporator.

shown in Table III. In order to verify the reliability of MIVM, the experimental data of activities[20] are listed in Table III for a comparison. It can be seen from Table III that the predicted activities of MIVM match well with the experimental data, and the predicting average relative deviation and the standard deviation were also calculated using the following equations, as shown in Table III:

$$S_i = \pm \frac{100}{n} \sum_{i=1}^{n} \left| \frac{a_{i,\exp} - a_{i,\text{pre}}}{a_{i,exp}} \right| \qquad [14]$$

$$S_i^* = \pm \left[\frac{1}{n} \sum_{i=1}^{n} \left[a_{i,\exp} - a_{i,\text{pre}} \right]^2 \right]^{1/2}, \qquad [15]$$

where $a_{i,\exp}$ and $a_{i,\text{pre}}$ are the experimental data and the predicted values of activity, respectively; and n is the number of experimental data. As can be seen from Table III, the predicting average relative deviations were ±0.2569 and ±0.1977 pct for Sn and Zn, and the standard deviations ±0.0016, ±0.0014, respectively, which indicates that the MIVM is reliable.

Based on the above analysis, the activity coefficients of Sn and Zn were also calculated in the temperature range of 873 K to 1273 K (600 °C to 1000 °C) (Table IV) for predicting separation coefficients and vapor–liquid phase equilibrium of Sn-Zn alloy system in vacuum distillation.

B. Separation Coefficients

The reason of separation of alloys by vacuum distillation is the composition difference between vapor phase and liquid phase. In order to demonstrate the feasibility and the separating degree of different elements in Sn-Zn alloy during vacuum distillation, separation coefficient,[23] *viz.* β, was introduced from theoretical derivation for Sn-Zn binary alloy, and it can be expressed as

$$\beta_{Zn} = \frac{\gamma_{Zn}}{\gamma_{Sn}} \cdot \frac{P_{Zn}^*}{P_{Sn}^*}, \qquad [16]$$

Table III. Comparison of the Predicted Values of MIVM with the Experimental Data[20] of Activities of Components Sn and Zn in the Liquid Alloy Sn-Zn at 750 K (477 °C)

$n = 9$	a_{Sn}			a_{Zn}	
x_{Sn}	MIVM	Exp.		MIVM	Exp.
0.1	0.272	0.274		0.924	0.924
0.2	0.383	0.383		0.873	0.874
0.3	0.453	0.450		0.826	0.828
0.4	0.514	0.511		0.771	0.773
0.5	0.578	0.577		0.700	0.701
0.6	0.648	0.648		0.608	0.607
0.7	0.726	0.726		0.492	0.490
0.8	0.811	0.811		0.351	0.350
0.9	0.903	0.903		0.186	0.186

$S_{Sn} = \pm 0.2569$ pct; $S_{Sn}^* = \pm 0.0016$.
$S_{Zn} = \pm 0.1977$ pct; $S_{Zn}^* = \pm 0.0014$.

Table IV. Activity Coefficients of Components of Sn-Zn Alloy at the Required Temperatures

| T (K)	x_{Sn}	0.1	0.2	0.3	0.4	0.5	0.6	0.7	0.8	0.9
873 (600 °C)	γ_{Sn}	1.973	1.569	1.337	1.198	1.112	1.059	1.027	1.010	1.002
	γ_{Zn}	1.017	1.058	1.115	1.183	1.257	1.333	1.409	1.482	1.549
973 (700 °C)	γ_{Sn}	1.605	1.379	1.236	1.144	1.084	1.046	1.022	1.000	1.001
	γ_{Zn}	1.011	1.038	1.076	1.122	1.172	1.224	1.277	1.329	1.378
1073 (800 °C)	γ_{Sn}	1.354	1.238	1.157	1.101	1.062	1.035	1.017	1.007	1.002
	γ_{Zn}	1.006	1.022	1.045	1.073	1.105	1.140	1.177	1.214	1.252
1173 (900 °C)	γ_{Sn}	1.171	1.128	1.092	1.064	1.043	1.026	1.014	1.006	1.001
	γ_{Zn}	1.002	1.010	1.045	1.034	1.052	1.072	1.096	1.123	1.153
1273 (1000 °C)	γ_{Sn}	1.032	1.036	1.035	1.031	1.026	1.019	1.012	1.005	1.002
	γ_{Zn}	0.999	0.999	0.999	1.001	1.006	1.014	1.027	1.046	1.072
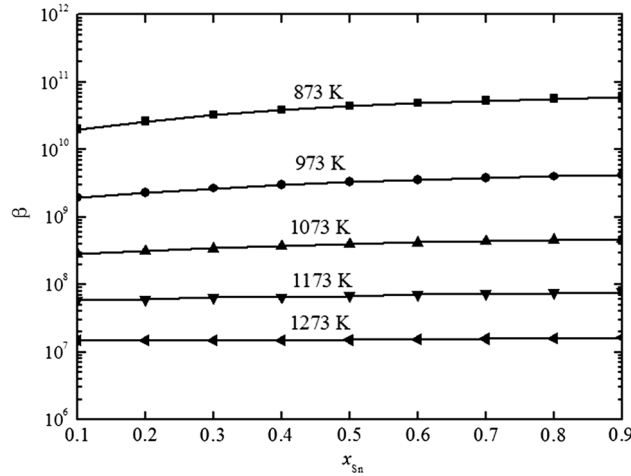
Fig. 2—Separation coefficients of Sn-Zn alloy system at different temperatures in vacuum distillation, predicted by MIVM.

where γ_{Sn} and γ_{Zn} are the activity coefficients of the Sn and Zn components, respectively; and P^*_{Sn} and P^*_{Zn} are the saturated vapor pressures of the Sn and Zn components, respectively. The saturated vapor pressures of pure Sn and Zn were available in Reference 23. The relationship between the mass fraction of Sn and Zn in the liquid phase and the vapor densities of Sn and Zn can be expressed as follows:

$$\frac{\rho_{Zn}}{\rho_{Sn}} = \beta_{Zn} \cdot \frac{\omega_{Zn}}{\omega_{Sn}}. \qquad [17]$$

The separation of Sn and Zn can happen while $\beta_{Zn} > 1$ or $\beta_{Zn} < 1$, but it cannot happen while $\beta_{Zn} = 1$.

Substituting the activity coefficients γ_{Sn} and γ_{Zn}, saturated vapor pressures P^*_{Sn} and P^*_{Zn} into Eq. [16], the separation coefficients at the required temperatures can be calculated (Figure 2). Figure 2 shows that the separation coefficients are far larger than 1 in the temperature range of 873 K to 1273 K (600 °C to 1000 °C), and it is shown that the content of Zn in the vapor phase is far larger than that of Sn, which indicates that Zn and Sn can be concentrated in the vapor and liquid phase, respectively, by vacuum distillation.

C. Vapor–Liquid Phase Equilibrium

The equilibrium composition diagram between vapor and liquid phase can describe precisely the elements distribution of metals in vacuum distillation process. It has an important instructive significance for both experimental and industrial production in the recycling and separation process of vacuum distillation. The present study has investigated the relationship between the vapor and liquid phase of $i - j$ alloy through calculating the vapor–liquid equilibrium composition.

For Sn-Zn alloy, the content of Zn and Sn in the vapor and liquid phase will be expressed with $\omega_{Zn,g}$, $\omega_{Sn,g}$, and $\omega_{Zn,l}$, $\omega_{Sn,l}$, respectively. Then the relationship between the mass fraction of Zn and Sn in the vapor and liquid phase can be represented as follows, respectively:

$$\omega_{Zn,g} + \omega_{Sn,g} = 1 \qquad [18]$$

$$\omega_{Zn,l} + \omega_{Sn,l} = 1. \qquad [19]$$

When the two phases are in equilibrium, the mass fraction of Sn in the vapor phase is related to the vapor densities of Zn and Sn as follows[23]:

$$\omega_{Sn,g} = \frac{\rho_{Sn}}{\rho_{Sn} + \rho_{Zn}} = \frac{1}{1 + (\rho_{Zn}/\rho_{Sn})}. \qquad [20]$$

Equations [16] and [17] were substituted into Eq. [20]. After rearranging, the mass fraction of Sn in vapor phase can be expressed as

$$\omega_{Sn,g} = \left[1 + \left(\frac{\omega_{Zn,l}}{\omega_{Sn,l}} \right) \cdot \left(\frac{\gamma_{Zn}}{\gamma_{Sn}} \right) \cdot \left(\frac{P^*_{Zn}}{P^*_{Sn}} \right) \right]^{-1}, \qquad [21]$$

where ω, γ, P^*, and β are the mass fraction, activity coefficients, saturated vapor pressure, and separation coefficient, respectively.

The relationship diagram of $\omega_{Sn,g}$–$\omega_{Sn,l}$ can be calculated by P^*, γ, and a series of $\omega_{Zn,l}/\omega_{Sn,l}$ at desired temperatures, i.e., the vapor–liquid equilibrium composition for the Sn-Zn system.

Substituting the activity coefficients γ_{Zn}, γ_{Sn}, saturated vapor pressure P^*_{Zn}, P^*_{Sn}, and a series of $\omega_{Zn,l}/\omega_{Sn,l}$ into Eq. [21], the vapor–liquid phase equilibrium of Sn-Zn
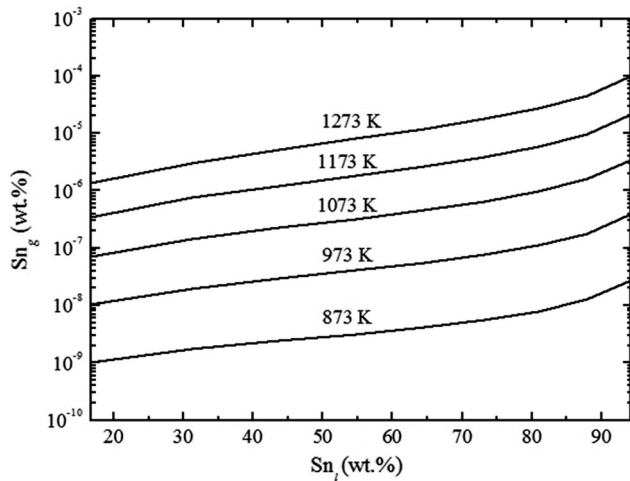
Fig. 3—Vapor–liquid equilibrium composition of Sn-Zn alloy system at the different temperatures.

alloy system can be easily calculated as shown in Figure 3 at the desired temperatures.

It can be seen from Figure 3 that the content of tin in the vapor phase was 0.000021 wt pct, while in the liquid phase, it was 90 wt pct at 1173 K (900 °C); it reached 0.000052 wt pct in the vapor phase, while in the liquid phase, it was 99.98 wt pct at 1173 K (900 °C). Figure 3 also shows that the content of tin in vapor phase increases quickly with the increasing distillation temperature and the mass fraction of tin in the liquid phase, the increasing tendency of the content of tin in the vapor phase can be explained by the fact that the vapor pressure of Sn increases as the temperature and the mass fraction of tin in the liquid phase increase.

D. Maximum Evaporation Rate

In order to further demonstrate that the separation of Zn from Sn by vacuum distillation is feasible from the standpoint of kinetics, the maximum evaporation rate was also calculated in this study. When the total chamber pressure is less than the saturated vapor pressure of a pure element and the mean free path of the vaporized molecule is greater than the distance between evaporator and condensing surface of the unit, the evaporation rate of the distilled element reaches maximum,[23] which can be expressed as

$$\omega_{max} = 2.624 \times 10^{-2} \times P_i^* \times \left(M/T\right)^{1/2} \times f, \quad [22]$$

where ω_{max} is the maximum evaporation rate, f is the distillation coefficient, M is the relative molecular mass of the distilled element, P_i^* is the saturated vapor pressure of pure metal in Pa, and T is the melt surface temperature in K, respectively. Supposing that the distillation coefficient $f = 1$, the maximum evaporation rate of Sn and Zn can be calculated from Eq. [22] in the temperature range of 873 K to 1273 K (600 °C to 1000 °C), as shown in Table V.

Table V. Maximum Evaporation Rate of Sn and Zn at Different Temperatures

T [K (°C)]	$\omega_{max,Zn}$ (g cm^{-2} min^{-1})	$\omega_{max,Sn}$ (g cm^{-2} min^{-1})
873 (600)	9.60	3.32×10^{-10}
973 (700)	4.78×10^{1}	2.10×10^{-8}
1073 (800)	1.73×10^{2}	6.10×10^{-7}
1173 (900)	4.98×10^{2}	9.93×10^{-6}
1273 (1000)	1.20×10^{3}	1.04×10^{-4}

It can be seen from Table V that the maximum evaporation rate of Zn and Sn increase exponentially with the increasing distillation temperature, and the maximum evaporation rate of Zn was several orders of magnitude greater than that of Sn at the same temperature. Therefore, Zn with high maximum evaporation rate will evaporates and concentrates into vapor phase, while Sn remains in the distillate. It is easy to separate Zn from Sn completely because the value of $\omega_{max, Zn}$ is $10^7–10^{10}$ times greater than that of $\omega_{max,Sn}$ in the temperature range of 873 K to 1273 K (600 °C to 1000 °C).

E. Experimental Results

The factors influencing the volatilization ratio of Zn were studied under different experimental conditions including distillation temperature, chamber pressure, and soaking time.

1. Effect of distillation temperature

The experiments were conducted between 873 K (600 °C) and 1273 K (1000 °C) in 100 K (100 °C) steps, maintaining the soaking time at 40 minutes, corresponding to the residual gas pressure of 15 Pa. The relationship between volatilization ratio of Zn and distillation temperature is shown in Figure 4(a). As shown in Figure 4(a), the volatilization ratio of Zn increases from 99.47 to 99.99 pct when the distillation temperature changes from 873 K to 1173 K (600 °C to 1000 °C). Nevertheless, it shows an incubation period for the volatilization ratio of Zn after 1173 K (900 °C). The increasing tendency of the volatilization ratio can be attributed to the fact that the saturated vapor pressure of Zn increases with the increasing distillation temperature.

2. Effect of soaking time

The object of the experiments in this series is to observe the influence of soaking time on the volatilization ratio of Zn. These experiments were carried out at 1173 K (900 °C) with chamber pressure of 15 Pa. Soaking times were changed from 20 to 60 minutes in 10 minutes steps. The experimental results are shown in Figure 4(b).

As shown in Figure 4(b), within 40 minutes, the volatilization ratio of Zn increased gradually as the soaking time was increased. For an increase in soaking time from 20 to 40 minutes, the volatilization ratio of
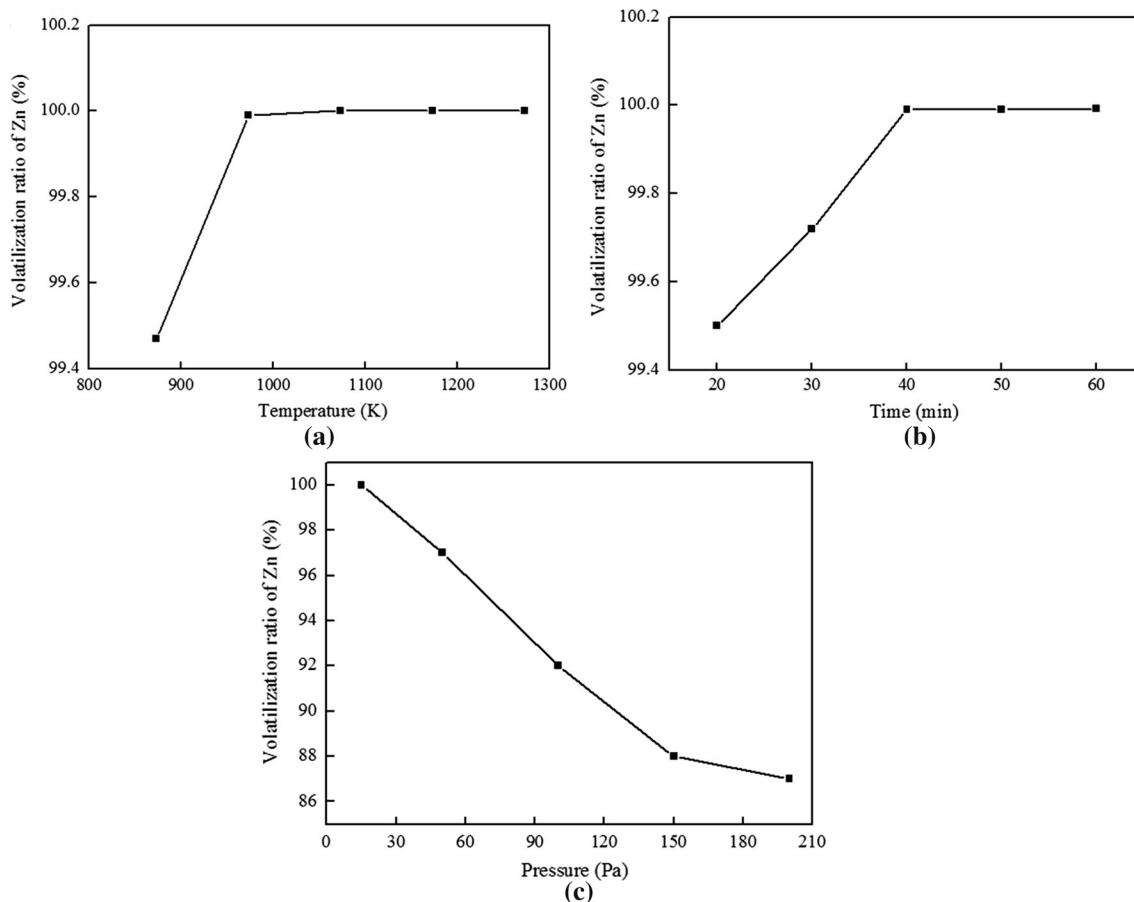
Fig. 4—Effects of (a) distillation temperature, (b) soaking time, and (c) chamber pressure on volatilization ratio of Zn.

Zn increased from 99.50 to 99.99 pct. When the soaking time was more than 40 minutes, the volatilization ratio remained constant as the soaking time was increased. After the soaking time of 40 minutes, prolonging the soaking time will result in more energy consumption, which comes to naught.

3. Effect of chamber pressure

The effect of chamber pressure on the volatilization ratio of Zn was investigated ranging from 15 to 200 Pa, at distillation temperature 1173 K (900 °C), and soaking time of 40 minutes. The relationship between volatilization ratio of Zn and chamber pressure is shown in Figure 4(c). As can be seen from Figure 4(c), the volatilization ratio of Zn decreases obviously as the chamber pressure is increased. When the pressure increases from 15 to 200 Pa, the evaporation percent of Zn correspondingly decreases from 99.99 to 87 pct. This means that the smaller the chamber pressure is, the higher the volatilizing ratio of Zn will be, but take into consideration of the critical pressure,[23] the chamber pressure is determined as 15 Pa.

4. Analysis of products

After vacuum distillation of Sn-Zn alloy, Sn was concentrated in the residue which was obtained from the graphite crucible, and Zn was evaporated into the volatile which was collected from the cold plate, as shown in Figure 5. The experimental condition and results are summarized in Table VI. Table VII gives the main chemical composition of residue and volatile when vacuum distillation was carried out at 1173 K (900 °C) for 40 minutes, with chamber pressure of 15 Pa and feeding amount of 120 g.

It can be seen from Table VII that the content of tin in the vapor phase was 0.001 wt pct, while in the liquid phase, it was 99.98 wt pct which is consistent with the predicted results.

In order to verify the predicting effect of MIVM, the experimental results and the predicted values of the MIVM were compared directly in Table VIII.

It can be seen from Table VIII that the predicted result for tin content in the vapor phase, viz. Sn(g), is in good agreement with the experimental data, although a deviation was observed. The experimental results of Sn content in the vapor phase is larger than the predicted values; the reasons may arise from the experimental conditions, such as the distillation temperature and chamber pressure were not controlled as well as enough. Meanwhile, the chamber pressure could not be controlled at an idea value. In addition, the prediction was based on the dynamic equilibrium condition. The experiments, however, were executed on a condition which could not reach equilibrium in the finite soaking time.

(a)   **(b)**

Fig. 5—The product of experiment: (*a*) residue; (*b*) volatile.

Table VI.   Summary of Experimental Condition and Results

Temperature [K (°C)]	Pressure (Pa)	Time (min)	Feeding Amount (g)	Volatile (g)	Residue (g)	Loss (g)	Volatilization Ratio of Zn (pct)
1173 (900)	15	40	120	76.8	42.8	0.4	99.99

Table VII.   Chemical Composition of Metallic Elements in the Residue and Volatile

Volatile				Residue				Loss	
Sn		Zn		Sn		Zn			
Mass (g)	Content (wt pct)	Mass (g)	Content (wt pct)	Mass (g)	Content (wt pct)	Mass (g)	Content (wt pct)	Mass (g)	Content (wt pct)
0.000768	0.001	76.7992	99.999	42.7923	99.98	0.007716	0.018	0.4	0.333

Table VIII.   Comparison of the Predicted Values and the Experimental Results of the Content of Sn in the Residue and Volatile at 1173 K (900 °C)

		Sn_g (wt pct)	
T [K (°C)]	Sn_l (wt pct)	Experimental	Predicted
1173 (900)	99.98	1.0×10^{-3}	5.2×10^{-5}

V.   CONCLUSIONS

1. Based on the MIVM, the activities of components of Sn-Zn alloy were predicted using only two parameters γ_i^∞ and γ_j^∞. The predicted activities of MIVM are in excellent agreement with the experimental data.
2. The separation coefficients of Sn-Zn alloy at the required temperatures were predicted using the MIVM, which indicates that Zn can be separated from Sn by vacuum distillation thoroughly. The vapor–liquid phase equilibrium of the Sn-Zn binary alloy in vacuum distillation was also predicted using MIVM. The predicted results show that the content of Sn in the vapor phase was 0.000052 wt pct, while in the liquid phase, it was 99.98 wt pct at 1173 K (900 °C).
3. The effect of distillation temperature, soaking time, and chamber pressure on volatilization ratio of Zn was investigated. The optimum operational condition [1173 K (900 °C), 40 minutes, and 15 Pa] was determined by series of experiments. The experimental results show that the content of Sn in the vapor phase was 0.001 wt pct, while in the liquid phase, it was 99.98 wt pct at the optimum condition.
4. The experimental results match well with the predicated values, which indicate that the MIVM is reliable for the prediction of vacuum distillation of Sn-Zn system. The present work extends previous investigations and provides a rigorous model on which to base refining simulations for Sn-based alloys.

REFERENCES

1. H.Y. Lee, J.K. Oh, and D.H. Lee: *Metall. Mater. Trans. B*, 1990, vol. 21B, pp. 455–61.
2. Y. Waseda and M. Issiki: *Purification Process and Characterization of Ultra High Purity Metals: Application of Basic Science to Metallurgical Processing*, Springer, New York, 2002.
3. S.T. Ali, K.S. Rao, C. Laxman, N.R. Munirathnam, and T.L. Prakash: *Sep. Purif. Technol.*, 2012, vol. 85, pp. 78–182.
4. L.X. Kong, B. Yang, B.Q. Xu, Y.F. Li, D.C. Liu, and Y.N. Dai: *Vacuum*, 2014, vol. 101, pp. 324–27.
5. T. Kato, M. Iizuka, T. Inoue, T. Iwai, and Y. Arai: *J. Nucl. Mater.*, 2005, vol. 340, pp. 259–65.
6. S.T. Ali, D.S. Prasad, N.R. Munirathnam, and T.L. Prakash: *Sep. Purif. Technol.*, 2005, vol. 43, pp. 263–67.
7. S.T. Ali, R.C. Reddy, N.R. Munirathnam, C. Sudheer, G. Anil, and T.L. Prakash: *Sep. Purif. Technol.*, 2006, vol. 52, pp. 288–94.
8. L. Zhan, Z.L. Qiu, and Z.M. Xu: *Sep. Purif. Technol.*, 2009, vol. 68, pp. 397–402.
9. A. Gopala, H. Kipphardt, R. Matschat, and U. Panne: *Mater. Chem. Phys.*, 2010, vol. 122, pp. 151–55.
10. D.P. Tao: *Themochim. Acta*, 2002, vol. 385, pp. 5–10.
11. L. Han, B. Yang, B.Z. Yang, Y.N. Dai, and D.C. Liu: *China Nonferr. Metall.*, 2007, vol. 4 (2), pp. 55–57.
12. L.X. Kong, B. Yang, Y.F. Li, B.Q. Xu, D.C. Liu, and G.B. Jia: *Metall. Mater. Trans. B*, 2012, vol. 43B, pp. 1649–56.
13. H.W. Yang, D.P. Tao, and Z.H. Zhou: *Acta Metall. Sin. (Engl. Lett.)*, 2008, vol. 21 (5), pp. 336–40.
14. D.P. Tao: *Themochim. Acta*, 2000, vol. 363, pp. 105–113.
15. D.P. Tao: *Metall. Mater. Trans. A*, 2004, vol. 35A, pp. 419–24.
16. H.W. Yang, B. Yang, B.Q. Xu, D.C. Liu, and D.P. Tao: *Vacuum*, 2012, vol. 86 (9), pp. 1296–99.
17. S. Poizeau, H. Kim, J.M. Newhouse, B.L. Spatocco, and D.R. Sadoway: *Electrochim. Acta*, 2012, vol. 76, pp. 8–15.
18. S. Poizeau and D.R. Sadoway: *J. Am. Chem. Soc.*, 2013, vol. 135, pp. 8260–65.
19. J.M. Newhouse, S. Poizeau, H. Kim, B.L. Spatocco, and D.R. Sadoway: *Electrochim. Acta*, 2013, vol. 91, pp. 293–301.
20. R. Hultgren, P.D. Desai, D.T. Hawkins, M. Geiser, and K.K. Kelley: *Selected Values of the Thermodynamic Properties of Binary Alloys*, ASM, Metals Park, 1973, p. 1335.
21. T. Iida and R.I.L. Guthrie: *The Physical Properties of Liquid Metals*, Clarendon Press, Oxford, 1988.
22. R. Ferro and A. Saccone: in *Structure of Solids*, V. Gerold, ed., VCH Verlagsgesellschaft, Weinheim, 1993.
23. Y.N. Dai and B. Yang: *Vacuum Metallurgy for Non-ferrous Metals and Materials*, Metallurgical Industry Press, Beijing, 2000, p. 40.